Direct determination of the interlayer van der Waals bonding force in 2D indium selenide semiconductor crystal

Tadao Tanabe, Chao Tang, Yohei Sato, and Yutaka Oyama

Citation: Journal of Applied Physics **123**, 245107 (2018); doi: 10.1063/1.5024313
View online: https://doi.org/10.1063/1.5024313
View Table of Contents: http://aip.scitation.org/toc/jap/123/24
Published by the American Institute of Physics

Direct determination of the interlayer van der Waals bonding force in 2D indium selenide semiconductor crystal

Tadao Tanabe,[a] Chao Tang, Yohei Sato, and Yutaka Oyama
Department of Materials Science, Graduate School of Engineering, Tohoku University, Aramaki-Aza Aoba 6-6-11-1021, Sendai 980-8579, Japan

(Received 31 January 2018; accepted 7 June 2018; published online 26 June 2018)

The interlayer van der Waals bonding force in crystalline InSe was directly measured using a mechanical test equipment. The bulk γ-InSe crystal was grown by the temperature difference method under controlled vapor pressure, a unique liquid phase solution crystal growth method with a low and fixed growth temperature. The measured bonding force in the crystal was 20.8 N/cm^2, which is greater than that in 2D crystalline GaSe. We also made theoretical discussion of the van der Waals forces in InSe, based on the fluctuations in the electron cloud distributions around the atoms. *Published by AIP Publishing*. https://doi.org/10.1063/1.5024313

I. INTRODUCTION

III-chalcogenide compounds, such as GaSe and InSe, have attracted more and more interest, and studies of their optical applications have been conducted.[1] Also, they have been proven to be outstanding candidates for exploring the frontier field of spintronics[2] and quantum hall effect.[3,4] We constructed some test equipment for a previous study of the interlayer van der Waals bonding forces in GaSe.[5] Indium Selenide is a typical two-dimensional (2D) III-chalcogenide semiconductor and has recently attracted much interest because of its novel optical and electrical properties.[6] A bandgap of about 1.3 eV gives it great potential to be applied in high efficiency solar energy conversion devices[7] and infrared detectors.[8] Also, because the density of the dangling bonds and the surface states in InSe are very low, it is also a promising material for the buffer layers in heterojunction devices.[9] Moreover, the transport properties confirm that InSe is an outstanding candidate for exploring the field of quantum confinement.[10]

Bulk InSe is one type of van der Waals III-chalcogenide crystal, in which many cleavable single layers consisting of two Se^{2-} anions and one $[In_2]^{4+}$ cation are stacked together and where the atoms combine with each other by covalent bonding to form a Se-In-In-Se structure. The bonding between the layers is mainly due to van der Waals forces. The special layered structure gives InSe its novel optical and electrical properties, so it is worthwhile exploring the interlayer structure of InSe.

Until now, although the electrical, optical, and thermal properties of InSe have been measured experimentally, there has only been a small amount of research done on the mechanical properties of III-chalcogenide compounds, conducted by means of nano-indentation tests and first principles calculations. However, the interlayer bonding strength cannot be measured by these approaches.[11] The mechanical properties, especially the van der Waals bonding force in InSe, are important for studying the interlayer structure and device fabrication processes, such as mounting and wire bonding.

In this study, we investigated layered structures of crystalline InSe grown by the temperature difference method under controlled vapor pressure (TDM-CVP),[12] by quantitatively measuring the interlayer van der Waals bonding forces in the crystals. TDM-CVP ensures that less interlayer defects are introduced. In our previous results, we added Te into the GaSe crystal to enhance the mechanical strength of samples. We suggest that it is the existence of heavy atoms that introduce larger van der Waals interactions; however, there are more defects such as grain boundaries and dislocations in the mixed crystals than in single crystals. The experiments on InSe confirmed that the main reason for the reinforcement of interlayer bonding force in III-chalcogenides is the van der Waals interaction but not any others such as the dislocation strengthening. A theoretical discussion of the van der Waals interlayer bonding forces in both InSe and GaSe was done, and the results were compared with the experimental ones. The theoretical discussion involved determination of the interlayer forces between two single layers by considering the bonding strength contributed by the van der Waals forces between planes of indium and selenium.

II. EXPERIMENTS

Despite the fact that most of the previous research on InSe had been conducted employing crystals grown by the Bridgman-Stockbarger technique,[13] our samples were grown using TDM-CVP, a unique solution growth method. A schematic diagram of TDM-CVP with temperature distribution is shown in Fig. 1. The temperature is controlled by the three independently adjusted electric furnaces, then the concentration of selenium differs from place to place in the crucible, and finally, the dispersion of selenium introduces the supersaturation in the bottom of crucible and lets crystals grow. The advantages of TDM-CVP are as follows: first, the growth can be conducted at a fixed temperature lower than the melting point of InSe, which ensures that there are less defects arising from the thermal motion of the molecules;

[a]Author to whom correspondence should be addressed: tadao.tanabe.b1@tohoku.ac.jp. FAX: +81-22-795-7329. TEL.: +81-22-795-7330.

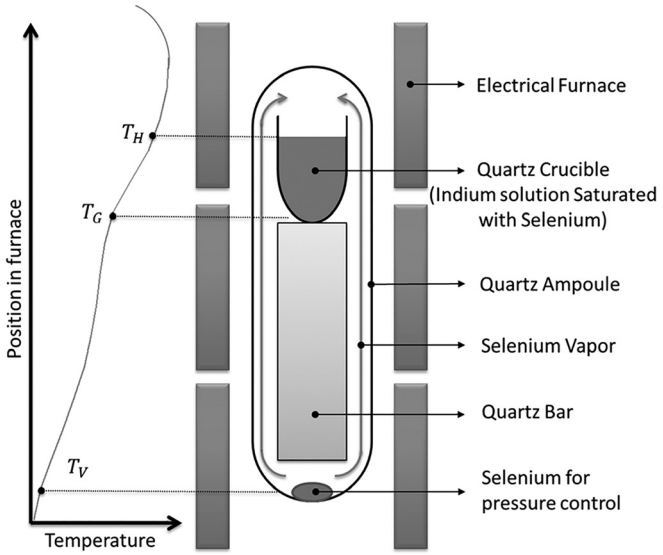

FIG. 1. Schematic diagram of the Temperature Difference Method under Controlled Vapor Pressure (TDM-CVP). The selenium vapor pressure can be controlled by Tv in this growth system. InSe crystals were grown due to super-saturation introduced by diffusion at the bottom of crucible.

second, because the InSe can be grown motionless by TDM-CVP, the nucleation in solution due to vibration caused by movement of the crucible can be avoided; finally, the stoichiometric composition and thus the quality of the crystal can be controlled by the stable selenium vapor pressure.

In TDM-CVP, it is the temperature gradient in the crucible that makes the selenium solute disperse and the crystal to grow. The growth conditions were as follows: the growth temperature was 582 °C and the temperature at the fluid level was 609 °C, which introduces a temperature gradient of 9 °C/cm in the crucible, and the selenium vapor pressure was kept at 65 Torr during growth. The growth took 14 days.

X-ray diffraction (XRD) measurements were conducted using a D8 ADVANCE (Bruker AXS Co., Ltd.) with CuKα_1 radiation. Moreover, backscattered Raman spectra were also obtained by implementing a STR250A (SEKI TECHNOTRON Co., Ltd.) with an excitation source at 532 nm. The Raman spectrum is shown in Fig. 2. With excitation at 532 nm, the absence of the Raman line at 200 cm^{-1} verified that our sample is γ-InSe. The results of the Raman spectra confirm that our samples were γ-InSe with R3m space group symmetry. From the XRD results for different parts of ingot, it was confirmed that the large part of the as-grown crystal is the InSe single crystal. As shown in Fig. 2, TEM images have been taken by JEM-2100F (JEOL Ltd.). The diffraction pattern of γ-InSe is shown in dark field images, and from the bright field image, it can be observed that there are no dislocations found in a large area. Our InSe is a single crystal but not a polycrystal. These results indicate that the oxidation has not occurred and our samples have favorable crystallinity. The samples used in this study were flacks peeled from the as-grown InSe ingot. The size of the InSe sample is about 8 mm, and the thickness is about 1 mm.

The van der Waals forces in the samples were measured using our unique mechanical test system shown in Fig. 3.[5] The InSe crystals are attached to the fixed stage using strong

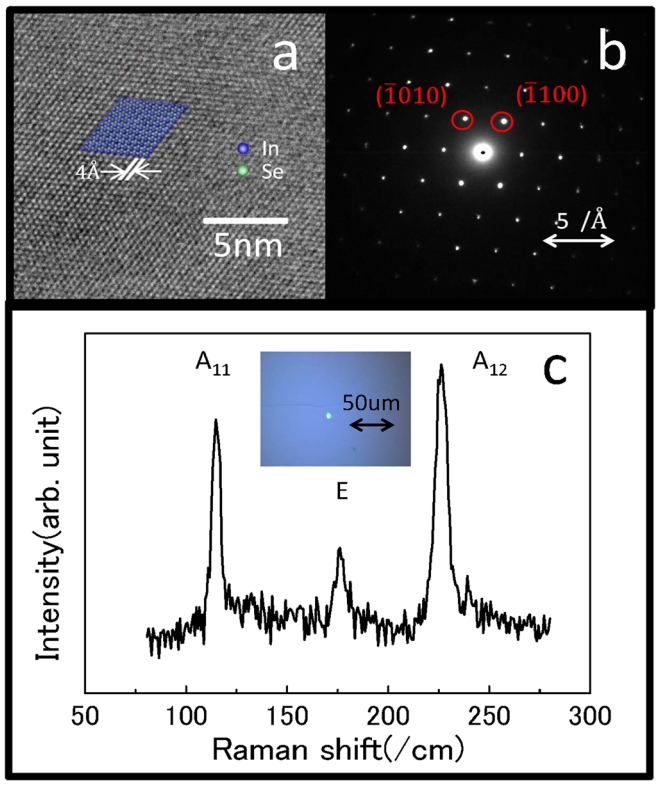

FIG. 2. Characterizations of the InSe crystal. (a) and (b) The bright and dark field images of TEM taken from the ⟨0001⟩ direction and (c) the Raman spectrum of the InSe crystal indicating that the tested sample is the γ-InSe crystal.

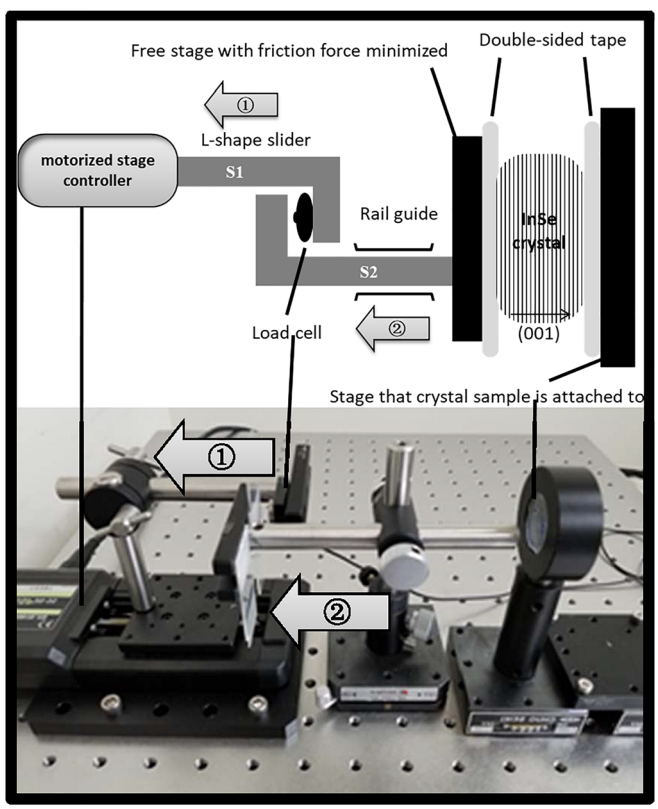

FIG. 3. Schematic diagram of the interlayer bonding force measurement system. InSe crystals were attached to the stage and cleaved by double-side adhesive tape. The load cell between two L-shape sliders recorded the force while samples being cleaved.

double-sided adhesive tape after cleavage of several surface layers. On the opposite side of the stage, there is an L-shaped slider (S2) with the same kind of double-sided tape. Another slider (S1) is drawn by a motorized stage controller at a speed of 1 mm/s. A SGSP20-35 (SIGMA KOKI Co., Ltd.) motor was used to cleave the samples. A LMA-A (KYOWA Co., Ltd.) load cell is placed between the two sliders (S1 and S2) to measure the tension when the samples are being tested. The precision of the load cell can reach 6×10^{-3} N. The adhesive force between the tape and the metal stage was measured in advance, and a value of 275 N/cm^2, which is far greater than that of the interlayer bonding force obtained from our experimental results, was obtained.

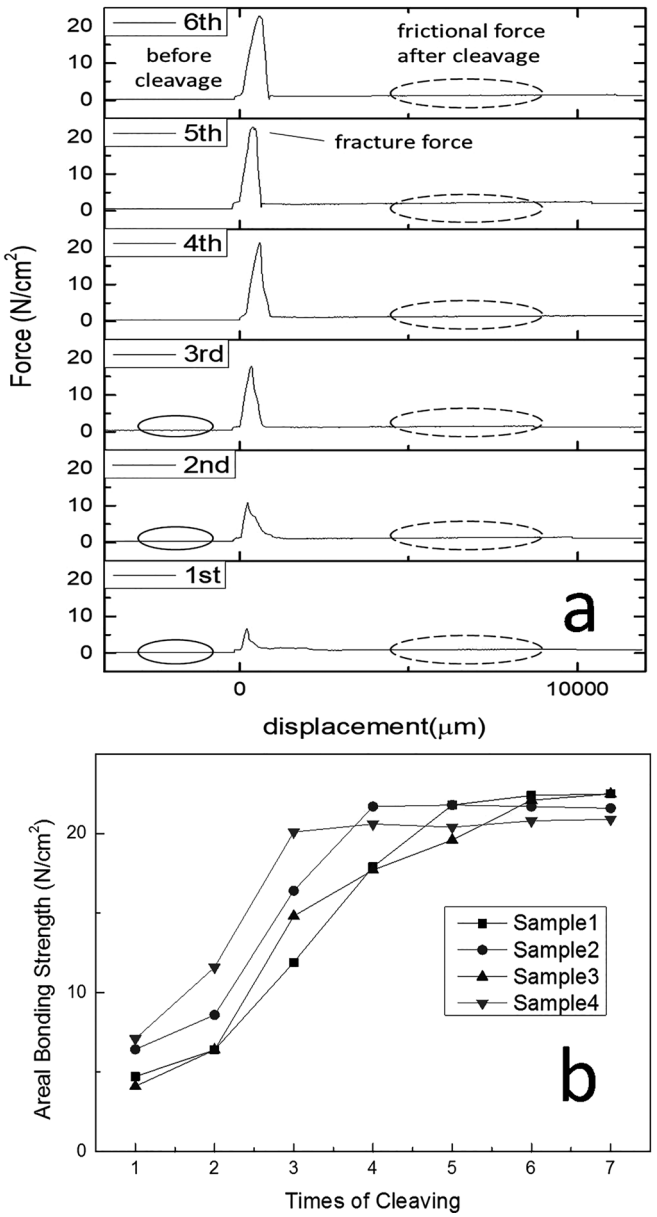

FIG. 4. (a). Average force per unit area measured by a strain gauge for the 1st to the 6th cleavage. The force reaches the maximum at the 4th cleavage. (b). Relationship between the bonding strength and the number of times each sample was cleaved. All the samples reached almost the same maximum value when numbers of cleavage increased.

III. RESULTS AND DISCUSSION

The InSe crystals were cleaved 6 times using the tension test equipment. Figure 4 shows the average force per unit area measured by the load cell from the first to the sixth time. These results suggest that the InSe crystals were elastically deformed before reaching the fracture force (σ_{max}). The force measurements circled by the dotted lines are attributed to the frictional force between the guide rail and the moving L-shape slider (σ_{fric}). The interlayer bonding force (σ_{bond}) was obtained by subtracting the frictional force from the fracture force [Eq. (1)]. The measured interlayer bonding force increases at first and then stays at almost the same value as the number of cleavage times increases. Although one can get a thinner InSe film by increasing the times of cleavage, here we only cleave the samples for several times to investigate the maximum of fracture force. This behavior can be explained as being due to some parts of the crystal already having fractures and there being defects, such as displacements, in the sample before the test. This would cause the interlayer strength to differ from place to place. The sample would rupture at the weakest parts, eventually leaving only the strongest parts. After the weaker parts had been removed, the measured force remained constant, and this can be considered to be the native interlayer bonding force in the crystal. The normalized interlayer bonding strength per unit area of crystalline InSe, compared with our previous results for crystalline GaSe,[5] is shown in Fig. 5. Forces of all the samples reach the maximum value. Here, the value shown in Fig. 5 is the average of data obtained from all samples, and an error is added according to the variance of results. The interlayer bonding force in InSe is far greater than that in GaSe

$$\sigma_{bond} = \sigma_{max} - \sigma_{fric}. \tag{1}$$

The van der Waals force between two atoms comprises a number of forces, i.e., the dispersion force, the induced dipole force, and the permanent dipole force, and can be expressed

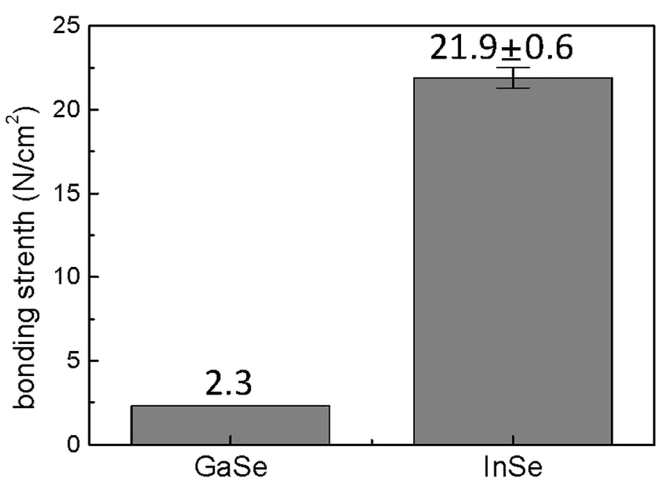

FIG. 5. Normalized bonding strengths of GaSe and InSe. The result of GaSe was published in our previous literature. The result of InSe is an average value of maximum value in Fig. 4(b) with an error bar of 4 samples.

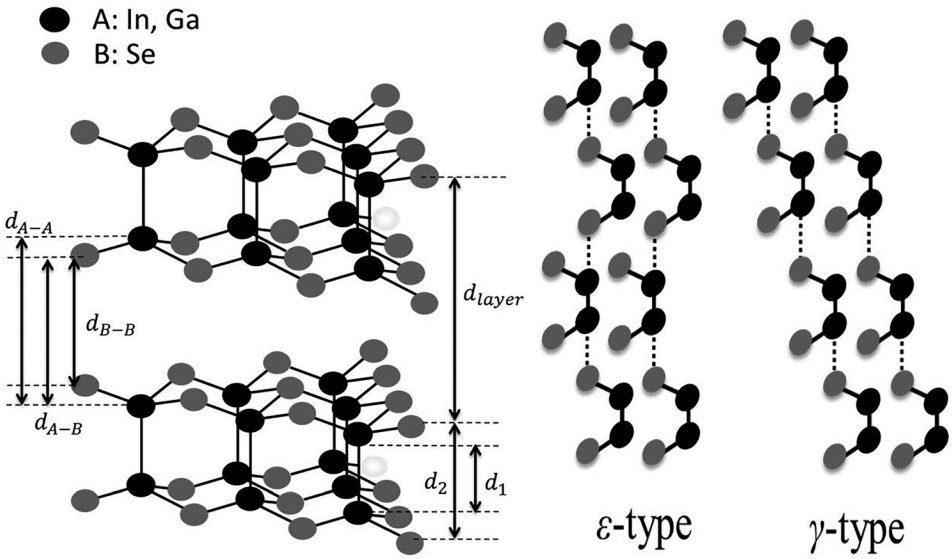

FIG. 6. Schematic diagram showing the structure of a layered III-chalcogenide semiconductor crystal. The left figure defines the distances listed in table. The right figure shows how the structure of polytype differs from each other.

by the following equation given by London[14] when the constituent atoms have no permanent dipole moment:

$$F_v = -\frac{1}{r^6}\left\{\frac{3}{4}\frac{h\alpha_1\alpha_2\nu_1\nu_2}{(\nu_1+\nu_2)}\right\}. \quad (2)$$

Here, $\boldsymbol{r}$ is the distance between the two atoms, α_1 and α_2 are the polarizabilities, and υ_1 and υ_1 are the vibration frequencies without the interatomic interaction. Then, the average van der Waals force per unit area between two large parallel planes (σ_p) with an area of S can be expressed by the following equation:[15]

$$\sigma_p(1,2) = \frac{\pi h\alpha_1\alpha_2\nu_1\nu_2}{8d_{12}^3}, \quad (3)$$

where d_{12} is the distance between the two parallel planes 1 and 2. A schematic diagram showing the structure of the layered III-chalcogenide semiconductor crystal is shown in Fig. 6. The black balls indicate the III-group metal atoms (A = In, Ga), and the grey balls indicate the chalcogen atoms (B = Se). In a single layer, two A planes are sandwiched between B planes. The thickness of a single layer (d_{layer}) can be calculated from the lattice constant. The distance between the A planes (d_1) and that between the B planes (d_2) within a single monolayer were obtained from a previously published report.[16] From these, we derived the distances between two A planes (d_{A-A}), two B planes (d_{B-B}), and the A and B planes (d_{A-B}) in neighboring layers. All these parameters for GaSe and InSe are listed in Table I.

The van der Waals force, which is proportional to r^{-6}, is a very short distance interaction. Thus, the van der Waals bonding force between two neighboring monolayers is mainly contributed by the nearest two A and B planes

TABLE I. The distance parameters for InSe and GaSe (unit: Å).

	d_{layer}	d_1	d_2	d_{AA}	d_{BB}	d_{AB}
InSe	8.320	2.740	5.300	5.580	3.020	4.300
GaSe	7.960	2.400	4.730	5.560	3.230	4.395

$$\sigma = \sum \sigma_p = \sigma_p(A,A) + \sigma_p(B,B) + 2\sigma_p(A,B). \quad (4)$$

The electric polarizability (α_1 and α_2) is the relative tendency of the charge distribution of the electron cloud around an atom to be distorted from its normal shape by an external electric field and this increases with the number of electrons.[17] It has been reported in other publications that the polarizabilities of In, Ga, and Se are 69, 54.9, and 26.2 in arbitrary units, respectively. In addition, the vibration frequencies of the atoms without interaction (υ_1 and υ_1) are proportional to the atomic mass. We use these values and Eq. (4) to compare GaSe with InSe. The results show that the van der Waals bonding force in InSe is nearly three times stronger than that in GaSe.

However, the difference between the experimental interlayer strengths in InSe and GaSe was far greater than this. Some possible reasons for this are as follows: first, our previous experiments were conducted using GaSe crystals belonging to the ε-polytype. However, the tests on InSe were conducted using crystals belonging to the γ-polytype. In fact, layered III-chalcogenide semiconductors always comprise a stable polytype due to the effects of Coulomb interactions,[18] which means that the Coulomb potentials of the two different polytypes are not the same. Moreover, there are more carriers belonging to the In atoms than the Ga atoms, which will introduce a greater Coulomb interaction. Furthermore, interactions other than the van der Waals force, such as ionic bonding and covalent bonding, contribute to the interlayer strength.

IV. CONCLUSION

In this study, we directly measured the interlayer bonding force in crystalline InSe and obtained a value of 20.8 N/cm^2. We compared this with the result obtained in a previous study for another kind of III-chalcogenide layered crystal. This was 2.3 N/cm^2 for GaSe, which shows that the van der Waals bonding force in InSe is stronger. Thus, there is

qualitative agreement between our results and our theoretical analysis of the interlayer van der Waals forces in InSe and GaSe.

ACKNOWLEDGMENTS

A part of this study is the result of "Fundamental Research and Human Resources Development Program for Nuclear Decommissioning related to Integrity Management of Critical Structures including Primary Containment Vessel and Reactor Building, and Fuel Debris Processing and Radioactive Waste Disposal" carried out under the Center of World Intelligence Project for Nuclear S&T and Human Resource Development by the Ministry of Education, Culture, Sports, Science and Technology of Japan.

[1]M. Suzuki, M. Kohda, S. Takasuna, S. Matsuzaka, Y. Sato, T. Tanabe, Y. Oyama, and J. Nitta, Jpn. J. Appl. Phys., Part 1 **57**, 020308 (2018).
[2]S. Takasuna, J. Shiogai, S. Matsuzaka, M. Kohda, Y. Oyama, and J. Nitta, Phys. Rev. B **96**, 161303(R) (2017).
[3]Z. R. Kudrynskyi, M. A. Bhuiyan, O. Makarovsky, J. D. G. Greener, E. E. Vdovin, Z. D. Kovalyuk, Y. Cao, A. Mishchenko, K. S. Novoselov, P. H. Beton, L. Eaves, and A. Patane, Phys. Rev. Lett. **119**, 157701 (2017).
[4]D. A. Bandurin, A. V. Tyurnina, G. L. Yu, A. Mishchenko, V. Zolyomi, S. V. Morozov, R. K. Kumar, R. V. Gorbachev, Z. R. Kudrynskyi, S. Pezzini, Z. D. Kovalyuk, U. Zeitler, K. S. Novoselov, A. Patane, L. Eaves, I. V. Grigorieva, V. I. Fal'ko, A. K. Geim, and Y. Cao, Nat. Nanotechnol. **12**, 223 (2017).
[5]T. Tanabe, S. Zhao, Y. Sato, and Y. Oyama, J. Appl. Phys. **122**, 165105 (2017).
[6]K. Xu, L. Yin, Y. Huang, T. A. Shifa, J. Chu, F. Wang, R. Cheng, Z. Wang, and J. He, Nanoscale **8**, 16802 (2016).
[7]S. E. Al Garni and A. A. A. Darwish, Sol. Energy Mater. Sol. Cells **160**, 335 (2017).
[8]Z. Chen, J. Biscaras, and A. Shukla, Nanoscale **7**, 5981 (2015).
[9]A. V. Velichko, Z. R. Kudrynskyi, D. M. Di Paola, O. Makarovsky, M. Kesaria, A. Krier, I. C. Sandall, C. H. Tan, Z. D. Kovalyuk, and A. Patanè, Appl. Phys. Lett. **109**, 182115 (2016).
[10]G. W. Mudd, S. A. Svatek, T. Ren, A. Patane, O. Makarovsky, L. Eaves, P. H. Beton, Z. D. Kovalyuk, G. V. Lashkarev, Z. R. Kudrynskyi, and A. I. Dmitriev, Adv. Mater. **25**, 5714 (2013).
[11]D. H. Mosca, N. Mattoso, C. M. Lepienski, W. Veiga, I. Mazzaro, V. H. Etgens, and M. Eddrief, J. Appl. Phys. **91**, 140 (2002).
[12]C. Tang, Y. Sato, T. Tanabe, and Y. Oyama, J. Cryst. Growth **495**, 54–58 (2018).
[13]A. Chevy, J. Cryst. Growth **67**, 119 (1984).
[14]F. London, Trans. Faraday Soc. **33**, 8b (1937).
[15]H. C. Hamaker, Physica **4**, 1058 (1937).
[16]H. Sun, Z. Wang, and Y. Wang, AIP Adv. **7**, 095120 (2017).
[17]E. V. Anslyn and D. A. Dougherty, *Modern Physical Organic Chemistry* (University Science Book, Sausalito, California, 2006).
[18]A. Zavrazhnov, A. Naumov, V. Sidey, and V. Pervov, Thermochim. Acta **527**, 118 (2012).